CHROM. 16,395

MEASUREMENT AND USE OF RETENTION DATA FROM HIGH-PERFORMANCE GRADIENT ELUTION

CONTRIBUTIONS FROM "NON-IDEAL" GRADIENT EQUIPMENT

M. A. QUARRY*, R. L. GROB* and L. R. SNYDER**,*
*Biomedical Products Department, E. I. du Pont de Nemours & Co., Concord Plaza, Wilmington, DE 19898
(U.S.A.)*
(Received October 25th, 1983)

SUMMARY

　　Equipment for high-performance liquid chromatographic (HPLC) gradient elution generally distorts the gradient selected by the operator, which in turn affects the retention of solutes separated by gradient elution. A theoretical analysis describes these gradient distortions as a function of equipment design and operating conditions. Comparisons of theory with experimental data show generally good agreement. As a result, it is now possible to select gradient conditions for minimal gradient distortion, or to correct for the effect of gradient distortion on solute retention. This will be shown in later papers to allow the use of gradient elution in new ways for more efficient method development and optimization of separation by HPLC.

INTRODUCTION

　　Gradient elution is widely applied in liquid chromatography to overcome certain general separation problems and resolve more efficiently certain kinds of samples (*e.g.*, refs. 1 and 2). Its applications include (1) optimal resolution and detection of compounds present in mixtures with a wide retention range, (2) selective adjustment of mobile-phase composition and selectivity for different parts of the chromatogram[3] and (3) rapid method development for isocratic separation by high-performance liquid chromatography (HPLC) (*e.g.*, refs. 2, 4 and 5). Gradient elution is particularly important for the separation of macromolecules such as proteins[6].

　　In these various applications of gradient elution, the relationship between sample retention and experimental conditions can be of major importance. A knowledge of this relationship allows the optimal use of gradient elution in separations that require this technique. This same theory of gradient retention *vs.* operating conditions

---

　* Chemistry Department, Villanova University, Villanova, PA 19085, U.S.A.
　** Lloyd R. Snyder, Inc., 2281 William Court, Yorktown Heights, NY 10598, U.S.A.

also allows the use of gradient runs to predict isocratic retention accurately as a function of the experimental conditions[6], permitting more rapid and convenient strategies for optimizing isocratic separations.

The present theory of retention in gradient elution[1] assumes that the gradient shape selected by the chromatographer is in fact delivered by the equipment to the head of the column. Actual gradients are invariably altered by the equipment and hence differ from the selected gradient, leading to differences in band retention for experimental *vs.* ideal gradient systems. Several workers have discussed the ability of different types of equipment to provide near-ideal gradients (*e.g.,* refs. 1, 2 and 7–10). However, no gradient systems are perfect in this respect, particularly for a wide range in potential applications (*e.g.,* with columns of ultra-small volume[11]). If it is accepted that present equipment generally yields gradients that are non-ideal to some degree, and if we desire to minimize these effects or correct for their contribution to the measured gradient retention times, then we require a better understanding of the relationship between gradient shape and equipment design and separation conditions. This is the aim of this paper. In the following paper[12] we present a similar analysis of gradient distortions that arise within the column, rather than as a result of non-ideal gradient equipment. Together these two papers provide a basis for (1) the more accurate use of theory to predict retention in gradient elution as a function of experimental conditions and (2) the use of gradient runs to obtain retention data for corresponding isocratic systems. Subsequent papers will show that this allows a considerably expanded use of gradient elution in diverse applications of the technique.

THEORY

The theory of retention for gradient *vs.* isocratic elution (same column, mobile phases) is given for linear solvent strength (LSS) conditions* in refs. 1 and 6. The latter treatment assumes ideal gradients, *i.e.,* gradients whose shapes are not disturbed by the equipment. We shall first review this theory for the case of ideal gradients, then we shall examine contributions to retention as a result of gradient non-ideality. A glossary of symbols used in this paper is given at the end of the following paper[12].

Ideal gradients

Under LSS conditions the mobile phase entering the column at time t will have a composition such that the solute capacity factor, k', in isocratic elution (same mobile phase) will be given by

$$\log k' = \log k_0 - b(t/t_0) \tag{1}$$

where k_0 refers to the value of k' at the beginning of the gradient ($t = 0$), t_0 is the column dead-time and b is a constant for the solute in question**. In reversed-phase

---

* LSS gradient systems generally provide optimal separations and are easily described mathematically.

** LSS gradients have also been defined as those where b is constant for all solutes, which in turn yields optimal or equivalent resolution throughout the chromatogram. The latter condition and the validity of eqn. 1 may be incompatible in a given gradient separation. Here we shall use the term LSS to mean only that eqn. 1 applies.

HPLC systems, isocratic retention data are given (approximately) as a function of mobile phase composition by

$$\log k' = \log k_w - S \varphi \qquad (2)$$

where k_w is the value (usually by extrapolation) for water as mobile phase, φ is the volume fraction of organic solvent in the mobile phase and S is a constant for a given solute and organic solvent. If φ varies linearly with time t during the gradient,

$$\varphi = \varphi_0 + (\varphi_f - \varphi_0) (t/t_G) \qquad (3)$$

then eqn. 1 is fulfilled and we have a LSS gradient. Here φ_0 and φ_f are the values of φ at the beginning and end of the gradient and t_G is the gradient time during which φ is varying. We can also derive the constant b in eqn. 1 from the above relationships:

$$b = S\Delta\varphi \, t_0/t_G \qquad (4)$$

where $\Delta\varphi = \varphi_f - \varphi_0$; for a 0–100% gradient, $\Delta\varphi = 1$. Eqns. 1–3 can be generalized to other HPLC systems by replacing φ with some function $f(\varphi)$ that is linear in log k'. Examples of $f(\varphi)$ are the solvent-strength parameter $\varepsilon°$ for adsorption chromatography, or $\log(C^{\pm})$ in ion-exchange chromatography; $(C^{\pm})$ refers to the concentration of ionic counter ion in the mobile phase[1].

For solutes not exhibiting size-exclusion effects[2,6], retention in LSS gradient elution with an ideal gradient is given by[1]

$$t_g = (t_0/b) \log(2.3k_0b + 1) + t_0 \qquad (5)$$

where t_g is the retention time of the solute under these conditions. When solute molecules are partially excluded from the particle pores by size-exclusion effects, eqn. 5 can be written as[6]

$$t_g = (t_0/b) \log[2.3k_0b(t_{sec}/t_0) + 1] + t_{sec} \qquad (6)$$

where t_{sec} is the observed value of t_0 for the solute in question, while t_0 applies to some other solute that is small enough to have access to the total pore volume of the packing particles (no size exclusion effect). Eqn. 6 is mainly of interest with regard to retention thermodynamics (as in ref. 6), rather than isocratic *vs.* gradient elution. We shall work with eqn. 5 in the remainder of this paper.

Causes and consequences of gradient nonideality

Gradient non-ideality can arise from the following effects: (1) solvent misproportioning and flow-rate errors due to pump design or faulty operation of the gradient system; (2) gradient delay due to the volume of the gradient mixer and connecting tubing, pump cylinder, etc.; (3) gradient distortion due to dispersion of the gradient in the mixer, connecting tubing, pump, etc. Gradient nonideality as a result of solvent misproportioning or flow-rate errors can give rise to gradients as in Fig. 1a, where the desired (ideal) gradient is shown by the dashed curve and the actual (non-ideal) gradient by the solid curve. Such gradients are typical of older designs of HPLC pumps, specifically those employing high-pressure mixing as discussed in ref.

10 and documented more recently by Engelhardt and Elgass[13]. In our experience this is less of a problem with many newer pumps that employ low-pressure mixing via proportioning valves for each solvent of the gradient. However, even with pumps of the latest design, compressibility effects commonly lead to fluctuations in flow-rate of ± 1–2% throughout the gradient, particularly when operating at higher pressures (150–300 bar) and with solvents whose mixtures exhibit large changes in viscosity over the gradient.

Gradient delay as a result of the volume of the system from mixer to column inlet is illustrated in Fig. 1b. In the simplest case, the delay time, t_D, is simply added on to the value of t_g from eqn. 5 (see below). However, for solutes eluting early in the gradient, the volume, V_D, of initial mobile phase (solvent A in the gradient A/B) associated with this gradient delay can cause pre-elution of the solutes; i.e., their partial migration along the column before the gradient arrives at the column inlet. This will result in smaller values of solute retention (t_g) relative to the case of no pre-elution (eqn. 10, below).

Gradient distortion as a result of dispersion within the system yields rounded gradients as in Fig. 1c. The degree of distortion at any time during the gradient can be characterized by the concentration difference, $\delta\varphi_m$, between actual and ideal gradients, as illustrated in Fig. 1d. This difference, $\delta\varphi_m$, in turn affects values of t_g.

Gradient misproportioning (Fig. 1a) is further discussed under Results and discussion, where our experience with the DuPont Model 8800 gradient system is reviewed. Gradient delay and its effect on solute retention are analyzed theoretically in the immediately following section and gradient dispersion is treated in the section after that.

In this and the following paper[12], it is convenient to express deviations between
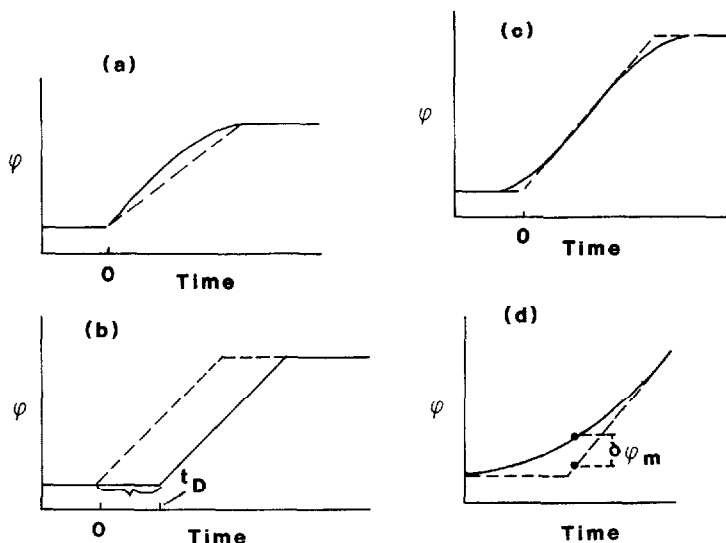

Fig. 1. Various hypothetical gradient distortions. – – – –, Ideal gradient; ———, actual gradient. (a) Gradient misproportioning; (b) gradient delay; (c) gradient dispersion; (d) same as (c), showing difference in concentrations φ vs. ideal gradient ($\delta\varphi_m$).

experimental and calculated (eqn. 10) values of t_g in terms of the value of φ at the time of elution of the band. The resulting difference in φ values, $\delta\varphi$, is given by

$$\delta\varphi = [(t_g)_{expt} - (t_g)_{calc}] (\Delta\varphi/t_G) \tag{7}$$

Experimental values of $\delta\varphi$ are in turn determined by the sum of the contributions, $\delta\varphi_i$, from individual causes of gradient nonideality:

$$\delta\varphi = \sum\delta\varphi_i \tag{7a}$$

Finally, values of $\delta\varphi_i$ are related to the average φ value for elution of the solute band. In the following manner, we can approximate the latter quantity $\bar{\varphi}$ by the value of φ at the band center when the band has migrated half-way along the column: From ref. 1, the value of t_g for elution of the band to the column midpoint is given by

$$(t_g)_{0.5} = (t_0/b) \log(1.15k_0b + 1) + 0.5t_0 \tag{8}$$

The value of φ at the column midpoint at the time $(t_g)_{0.5}$ is then related[1] to the latter quantity by

$$\bar{\varphi} = (\Delta\varphi/t_G) [(t_g)_{0.5} - 0.5t_0] + \varphi_0 \tag{9}$$

Gradient delay and solute pre-elution

Gradient delay without solute pre-elution (see Fig. 1b) simply adds the quantity t_D to t_g from eqn. 5:

$$t_g = (t_0/b) \log(2.3k_0b + 1) + t_0 + t_D \tag{10}$$

If k_0 is not very large (<50) and/or $t_D/t_0 > 1$, elution of solute bands can occur during passage of the volume $V_D = t_DF$ through the band after it is injected on to the column (F is flow-rate of the mobile phase). We can calculate the effect of solute pre-elution on t_g as follows. The fractional migration, x, of the solute band along the column during pre-elution is given by*

$$x = t_D/t_0k_0 \tag{11}$$

The retention time, t_g, for the solute is

$$t_g = t_D + t_0 + t_g^x \tag{12}$$

where t_g^x is the quantity $t_g - t_0$ for a column of length $1 - x$ times the actual column length (other conditions being the same). For a column of fractional length $1 - x$, values of t_0 (equal t_0^x) and b (equal b^x) relative to values for the original column can

---

* Note that if $t_D = t_0k_0$, $x = 1$ and the retention time, t_R, of the band is then t_0k_0 plus t_0 for the column dead volume.

be calculated: $t_0^x = (1 - x)t_0$ and $b^x = (S\Delta\varphi/t_G)t_0^x = (1 - x)b$. These latter quantities can be substituted for t_0 and b, respectively, in eqn. 10:

$$t_g^x = (t_0/b) \log[2.3k_0b(1 - x) + 1] \tag{13}$$

Combination of eqns. 12 and 13 then yields a final expression for t_g with gradient delay and pre-elution accounted for:

$$t_g = (t_0/b) \log[2.3k_0b(1 - x) + 1] + t_D + t_0 \tag{14}$$

Eqn. 14 can be further simplified to give an insight into the conditions required for significant pre-elution to occur. Let quantities a and c be defined as $a = 1 + 2.3k_0b$ and $c = 2.3k_0b$. Then eqn. 14 can be written as

$$t_g = (t_0/b) \log(a - cx) + t_D + t_0 \tag{15}$$

The change in t_g with x (when $x \ll 1$) is

$$(dt_g/dx) = -t_0c/2.3ab \tag{16}$$

The quantity $\delta\varphi_p$ ($\delta\varphi_i$ as a result of pre-elution) is

$$\delta\varphi_p = dt_g\Delta\varphi/t_G \tag{17}$$

which for small values of x is (eqns. 16 and 17)

$$\delta\varphi_p = (\Delta\varphi/t_G) (-t_0cx)/2.3ab \tag{18}$$

Substituting the above expressions for a and c into eqn. 18 gives finally (with eqns. 4 and 11)

$$\delta\varphi_p = bt_D/St_0(1 + 2.3k_0b) \tag{19}$$

For values of $k_0b \geqslant 3$, the latter expression is well approximated by

$$\begin{aligned} \delta\varphi_p &\approx (\Delta\varphi/2.3k_0b) (t_D/t_G) \\ &= (1/2.3Sk_0) (t_D/t_0) = (V_D/V_m)/2.3Sk_0 \end{aligned} \tag{20}$$

where V_m is the dead volume of the column. For example, consider the separation of a sample of molecular weight 200–500 with a methanol- or acetonitrile–water gradient ($S \approx 3$), a gradient system similar to that used here ($V_D = 5.5$ ml), and a 15×0.46 cm I.D. column ($V_m \approx 2$ ml). In this case the quantity $\delta\varphi_p$ is equal to about $0.4/k_0$. Therefore, an error in t_g equivalent to $\delta\varphi_p = 0.005$ requires a minimum value of k_0 equal to 80. Smaller values of k_0 give rise to proportionately larger errors in t_g (eqn. 20). Likewise, columns of smaller volume (smaller V_m) or with larger values of t_D also yield proportionally larger errors.

Gradient dispersion

In high-pressure gradient devices[1] the two solvents A and B are combined in a mixer of volume V_M, and the contents of the mixer are fed to the column inlet. If the volume of the mixer is large relative to the volume of tubing that connects the mixer and the column, the composition of the mobile phase entering the column can be approximated by the composition φ within the mixer. This is the simplest case to analyze, and we shall examine it first. We shall assume a linear gradient as in Fig. 1, with the mobile phase composition changing from water ($\varphi = 0$) to pure organic ($\varphi = 1$), i.e., $\Delta\varphi = 1$. We shall consider other situations ($\Delta\varphi < 1$) later. The composition φ_i of mobile phase (total) fed to the mixer can be given by

$$\varphi_i = (t/t_G) = (V/V_G) \tag{21}$$

A mass-balance equation can be written for the amount of organic solvent entering and leaving the mixer at any time:

$$(V/V_G)\,dV - \varphi dV = V_M\,d\varphi \tag{22}$$

The first term in eqn. 22 represents the influx to the mixer, the second term is the effluent from the mixer and the last term represents the increase in organic solvent within the mixer. Integration of eqn. 22 yields

$$\varphi = C\,e^{-V/V_M} + (V - V_M)/V_G \tag{23}$$

The constant C can be evaluated from the boundary condition $\varphi = 0$ when $V = 0$: $C = V_M/V_G$. Therefore

$$\varphi = (V_M/V_G)\,e^{-V/V_M} + (V - V_M)/V_G \tag{24}$$

The quantity $\delta\varphi_m$ (see Fig. 1d) is then

$$\delta\varphi_m = (V_M/V_G)\,e^{-V/V_M} \tag{25}$$

Eqn. 25 applies only for $V \gg 0$, because for $V < 0$ (before the gradient starts) the value of φ_i is zero for all values of V, and eqn. 21 does not apply. That is, end effects limit the range of applicability of eqn. 25. These end effects can be eliminated by integrating the case corresponding to $\varphi_i = 0$ for $V < 0$ and $\varphi_i = V/V_G$ for $V \geq 0$. The resulting integration was carried out for various model cases (varying values of V_M/V_G) by numerical means, and it was confirmed that eqn. 25 is accurate for $V \geq V_M$, but not for $V < V_M$. However, for the latter case ($V < V_M$) the results of numerical integration could be fit to an empirical expression:

$$\delta\varphi_m = (V_M/2.72\ V_G)\,e^{2.5(V - V_M)/V_M} \tag{26}$$

When V approaches V_G, eqn. 25 again fails. However, the end of the gradient is symmetrical compared with its beginning, in the following sense: $\delta\varphi_m$ for a value V in the first half of the gradient $= -\delta\varphi_m$ for value ($V - V_G$) in the second half.

Thus, $\delta\varphi_m = 0$ near the middle of the gradient and $\delta\varphi_m$ at $V = V_M$ equals $-\delta\varphi_m$ at $V = (V_G + V_M)$. Examples of values of $\delta\varphi_m$ calculated in this fashion are shown in Table I, for $V_M/V_G \leqslant 0.20$. Fig. 2 shows calculated gradient shapes (solid curves) at the beginning and end of the gradient for $V_M/V_G = 0.05$ (a), 0.1 (b) and 0.2 (c). The dashed curves in each instance show the shape of the ideal (undistorted) gradient after correction for dwell time.

For larger values of V_M/V_G and more severely distorted gradients, eqns. 25 and 26 no longer apply because end effects (at $V = V_M$ and $V_M + V_G$) now affect the entire gradient. Values of $\delta\varphi_m$ in Table I for these cases ($V_M/V_G > 0.2$) were determined experimentally, after confirming that eqns. 25 and 26 describe experimental gradient shapes within experimental error for $V_M/V_G \leqslant 0.2$.

Values of $\delta\varphi_m$ are dependent only on V_M/V_G, V/V_G and $\Delta\varphi$, as indicated in Table I. This can be seen from the form of eqns. 25 and 26 and the preceding discussion. For an example of the calculation of $\delta\varphi_m$, see Appendix I in the following paper[12].

More complex gradient systems

The preceding discussion of gradient dispersion assumes that only the gradient

TABLE I

CALCULATED ERROR IN ACTUAL GRADIENTS AS A FUNCTION OF V, V_M AND V_G (DUE TO GRADIENT DISPERSION)

Calculated by combination of eqns. 25, 26 plus numerical integration and experimental gradient data (see text).

$(V - V_D)/V_G{}^*$	Error in φ ($\delta\varphi_m/\Delta\varphi$) for various values of V_M/V_G						
	0.8	0.4	0.2	0.1	0.05	0.02	0.01
−0.2			0.006				
−0.1			0.021	0.000			
−0.05			0.039	0.011	0.000	0.000	0.000
0.0	0.34	0.119	0.074	0.037	0.018	0.007	0.004
0.05	0.33	0.106	0.057	0.022	0.007	0.002	0.000
0.10	0.31	0.092	0.045	0.014	0.003	0.000	0.000
0.15	0.29	0.082	0.035	0.008	0.001	0.000	0.000
0.20	0.27	0.071	0.027	0.005	0.000	0.000	0.000
0.30	0.22	0.058	0.016	0.002	0.000	0.000	0.000
0.40	0.17	0.050	0.010	0.001	0.000	0.000	0.000
0.50	0.11	0.043	0.006	0.000	0.000	0.000	0.000
0.60	0.05	0.026	0.004	0.000	0.000	0.000	0.000
0.70	−0.02	−0.002	0.000	0.000	0.000	0.000	0.000
0.80	−0.08	−0.040	−0.004	0.000	0.000	0.000	0.000
0.85	−0.11	−0.065	−0.012	0.000	0.000	0.000	0.000
0.90	−0.15	−0.090	−0.021	0.000	0.000	0.000	0.000
0.95	−0.19	−0.120	−0.039	−0.011	0.000	0.000	0.000
1.00	−0.22	−0.150	−0.074	−0.037	−0.018	−0.007	−0.004
1.05			−0.057	−0.022	−0.007	−0.002	0.000
1.10			−0.045	−0.014	−0.002	0.000	0.000
1.20			−0.027	−0.005	−0.000	0.000	0.000
1.40			−0.010	0.001	0.000	0.000	0.000

* $V_D = V_M$ when only the mixing vessel contributes to V_D.

mixing chamber contributes to gradient nonideality. In modern low-pressure mixing systems there are several elements that are individually similar to mixing chambers in being able to distort the shape of the final gradient. Thus, in addition to the low-pressure mixer, there are the pump cylinders, connecting tubing that joins the mixer, pump and column, plus in-line frits and filters. Each of these elements contributes additionally to the dispersion of the gradient curve.

For the case of several well-mixed vessels in series, the quantity V_M^2 is equal to the dispersion variance of the total system[1]. The resulting overall value of V_M for a series of mixing vessels i of volume V_i is then

$$V_M^2 = \sum_{}^{n} V_i^2 \tag{27}$$

The corresponding delay volume, V_D, is given by

$$V_D = \sum_{}^{n} V_i \tag{28}$$

Therefore, a total (actual) volume V_D apportioned among more than one mixing vessel yields the same delay volume (V_D) as for a single mixing vessel, but a lesser dispersion of the actual gradient (smaller value of V_M).

In the case of connecting tubing, the corresponding dispersion volume, V_C (equivalent to V_M), can be expressed by the Taylor equation[15] as

$$V_C^2 = V_c \, d_t^2 \, F/96 \, D_m \tag{29}$$

where V_c is the actual volume of liquid contained within the tube (equal to $\pi L \, d_t^2/4$), d_t is the inner diameter of the tube, F is the flow-rate of mobile phase through the tube and D_m is the average diffusion coefficient of solvents within the mobile phase. Typically, D_m will be about $5 \cdot 10^{-5}$ cm^2/sec, and V_C^2 will be about 0.002–0.04 ml^2 per meter of tubing when $d_t = 0.030$ in. (0.08 cm), for flow-rates of 0.2–4 ml/min. Eqn. 29 overestimates V_C for higher flow-rates and shorter lengths of tubing[16], but this effect can be ignored for typical gradient systems.

In the case of well designed frits and filters, which can be described as packed mixing vessels, the value of V_M will typically be much smaller than the volume of each such element, and the dispersion within these devices can be ignored in comparison with the dispersion of the gradient mixing chamber.

EXPERIMENTAL

Equipment

The HPLC system was a DuPont 8800 liquid chromatograph (DuPont, Wilmington, DE, U.S.A.) equipped with a Model 860 fixed-wavelength (254 nm) photometric detector and heated column compartment. A mixing chamber of current (1983) design was used, and a Mott CRT 6150 in-line filter (Mott Metallurgical, Farmington, NM, U.S.A.) was added. The recorder was an HP 7131A strip-chart recorder (Hewlett-Packard, San Diego, CA, U.S.A.).

Reagents

Solvents were HPLC-grade tetrahydrofuran (THF) and acetonitrile (J. T. Bak-

er, Jackson, TN, U.S.A.). A Milli-Q system with Organex-Q cartridge (Millipore, Bedford, MA, U.S.A.) was used for water purification. Solvents were degassed by helium sparging, prior to and during use.

Chromatographic conditions

Flow-rates were measured at various mobile phase compositions using a calibrated volumetric flask. The maximum flow-rate error was 2% over the gradient range studied. To determine the shape of gradients delivered to the column, analog gradient curves were obtained by adding a low concentration of a UV absorber (acetone or toluene) to one portion of solvent. Supplemented and unsupplemented
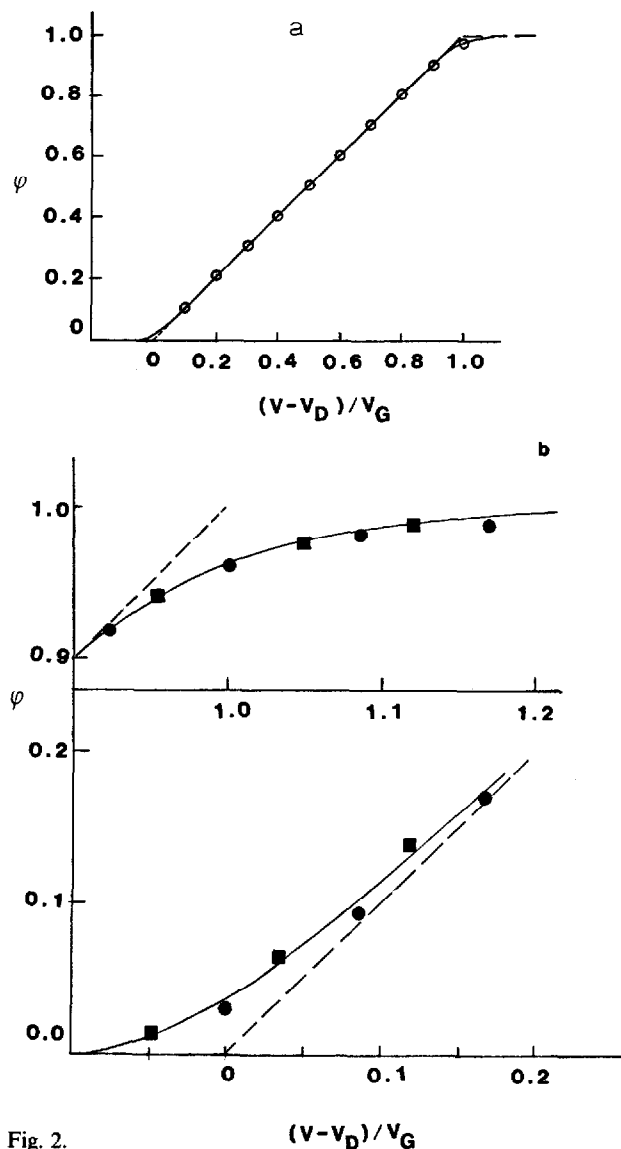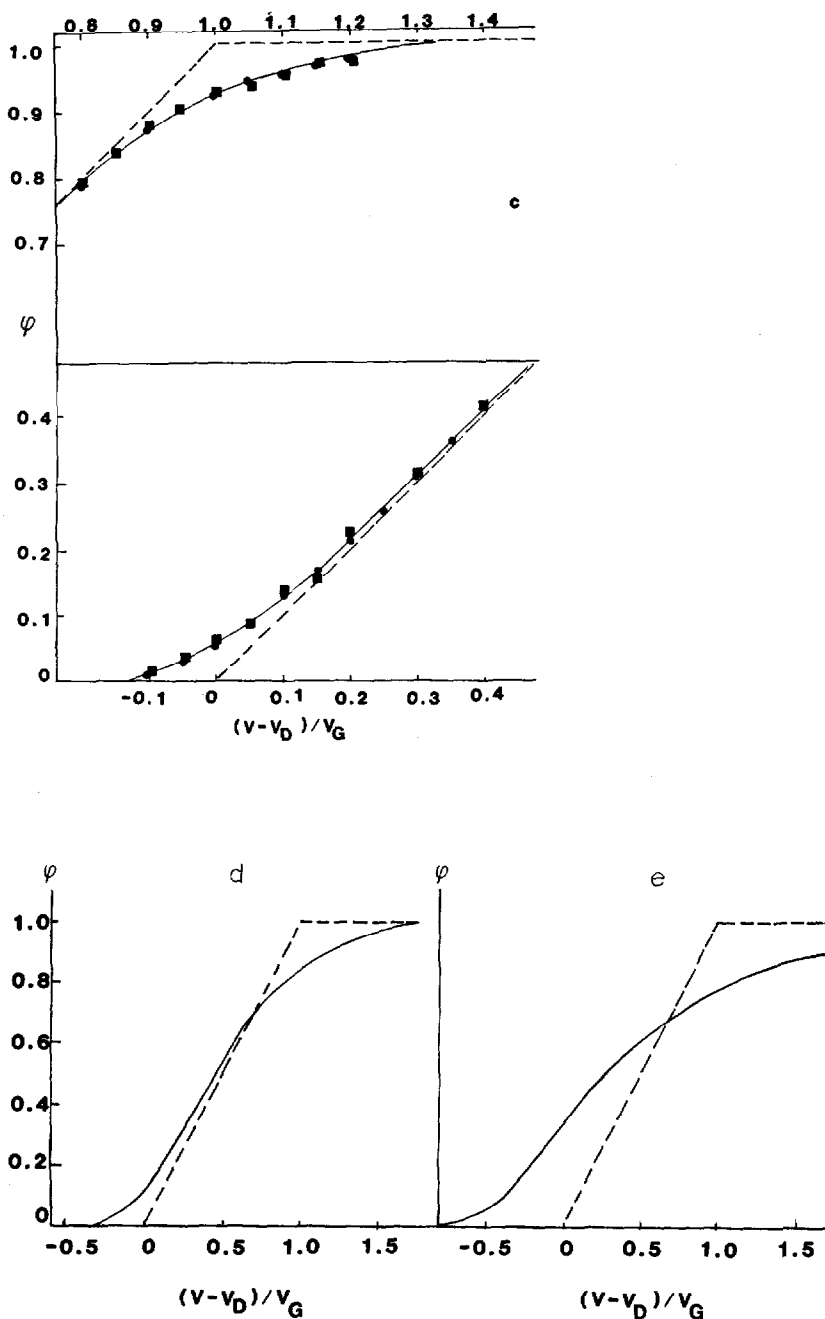

Fig. 2.

Fig. 2. Experimental *vs.* calculated (eqns. 25 and 26) gradients for acetonitrile–water mobile phase. (a) V_G = 40 ml, V_M/V_G = 0.05; (○, 2.0 ml/min, experimental data); – – –, ideal gradient; ———, calculated (eqns. 25 and 26). (b) V_G = 20 ml, V_M/V_G = 0.10; ●, 0.5 ml/min; ■, 2.0 ml/min; otherwise as in (a). (c) V_G = 10 ml, V_M/V_G = 0.20; otherwise same as in (b). (d) V_G = 5 ml, V_M/V_G = 0.40; ———, experimental curve, – – –, ideal curve. (e) V_G = 2.5 ml, V_M/V_G = 0.80; otherwise as in (d).

solvents were then used to form the gradient, with the column replaced by 5 ft. of 0.01 in. I.D. stainless-steel tubing. Flow-rates were varied from 0.2 to 10 ml/min, and gradient times were changed from 5 to 80 min. For other information, see the Experimental section of the following paper[12].

RESULTS AND DISCUSSION

A major aim of this study was to compare theory with experiment and to examine the effects of non-ideal gradients on measured retention times, t_g. In this section we shall develop guidelines for avoiding gradient nonideality such that significant changes in t_g result. We shall also discuss the correction of experimental t_g values for such effects.

Solvent misproportioning and flow-rate errors
Recent gradient devices featuring low-pressure mixing are generally free from major problems with solvent misproportioning. Unlike the high-pressure mixing systems of the 1970s (*e.g.*, Chapter 3 in ref. 2), low-pressure systems can provide accurate proportioning over the entire gradient range, not just for $0.05 < \varphi < 0.95$. In any case, a given gradient system can be tested for the shape of the gradient provided, as described under Experimental. Significant problems in solvent misproportioning will show up as a ripple on what should be a smooth, continuous curve, or as major deviations between the observed and expected gradient. No such problems were encountered with the DuPont 8800 instrument.
Once the proper gradient is generated in the mixer, this gradient is delivered by the HPLC pump to the column. Modern pumps provide compressibility corrections (Chapter 3 in ref. 2) to compensate for this major source of error in pumping
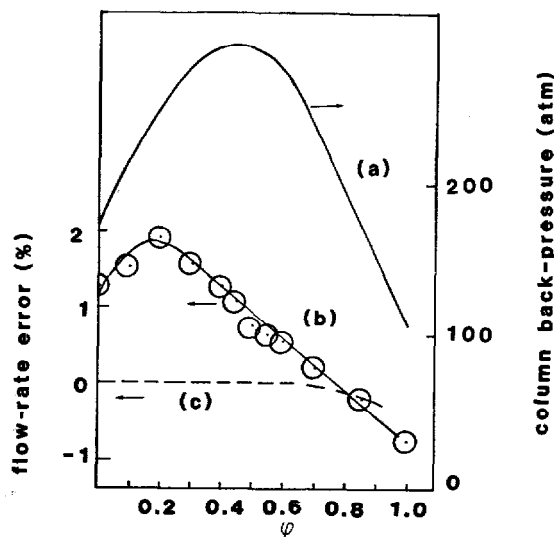

Fig. 3. Flow-rate errors for Model 8800 as a function of back-pressure. (a) Back-pressure *vs.* φ for runs of curve (b), ———; (b) flow-rate error *vs.* φ (THF–water mixtures, 2 ml/min, 25-cm column), O experimental data; (c) flow-rate error at lower back-pressure (same mobile phases, larger-particle column), – – –.

at high column back-pressures. However, these corrections are not exact, as illus-
trated for the present HPLC system in Fig. 3. Here we show the error in flow-rate for
different values of φ, the volume fraction of THF in THF–water mixtures. The circles
(b) are the experimental errors found when pumping at 2 ml/min into a 25 × 0.46
cm I.D. column of 5-μm particles. The solid curve (a) shows the corresponding back-
pressure on the pump. It is clear that these small errors in flow-rate roughly track
the column pressure, as theory predicts for errors due to partially compensated com-
pressibility effects. The dashed curve (c) shows the pumping errors for a lower back-
pressure (9–17 bar), created by using a 25 × 0.46 cm I.D. column of 30-μm particles
(flow-rate 2 ml/min). In the last case (curve c) the error in flow-rate is never greater
than 0.2%.

HPLC gradient separations usually involve pressures below 200 bar, and Fig.
3 suggests that in this case flow-rate errors should be less than 2% absolute. Consider
next the effect of such pumping errors on gradient retention times, t_g. Values of t_g
are given by eqn. 5, which is a function of column dead-time, t_0. A change in flow-
rate causes an inversely proportional change in t_0. In the following paper[12] it is
shown that an error in t_0 of x min results in an equal error in t_g (x min). We can
define the relative error in t_g due to error (δF) in flow-rate as in eqn. 7:

$$\delta\varphi_f = (\text{error in } t_0) \, \Delta\varphi/t_G$$
$$= (-\delta F/F)t_0\Delta\varphi/t_G \tag{30}$$

For optimized gradient runs in reversed-phase systems[1,2], t_0/t_G will be close to a
value of 0.05, and $\Delta\varphi$ will be about 1. This means that a 2% error in flow-rate (value
of $-\delta F/F$) will result in an error $\delta\varphi_f$ equal to about 0.001, i.e., negligible in most
instances. Further, this maximum error would be reduced by averaging of flow-rate
errors during the gradient run (see Fig. 3).

Gradient delay and solute pre-elution

The gradient delay time, t_D, for a given run will be the sum of two contribu-
tions: (a) the volume of the gradient system V_D (beginning with the mixer and ex-
tending to the column inlet) divided by flow-rate F, plus (b) the delay time t_d between
the initiation of the gradient by the operator or microprocessor and the actual re-
sponse of the gradient system. Thus

$$t_D = V_D/F + t_d \tag{31}$$

The apparent delay volume, V'_D, can then be defined, $V'_D = t_D F$, which combines
with eqn. 31 to give

$$V'_D = V_D + t_d F \tag{32}$$

Experimental values of V'_D from a given gradient system should agree with values
from eqn. 32. This is tested in Fig. 4 for the present system; experimental values of
V'_D are plotted against F as circles, and the vertical lines through each point represent
the variability (1 S.D.) of each value (replicate measurements). The straight line is a
best fit of eqn. 32 to these points, based on $t_d = 0.05$ min. The latter value represents
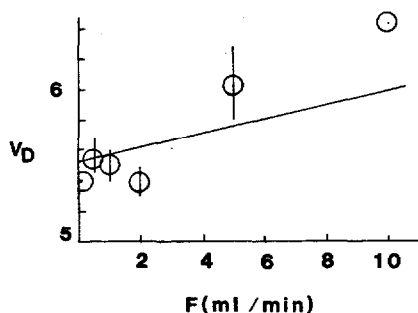
Fig. 4. Measured values of delay volume, V_D, as a function of flow-rate. Acetonitrile–water mixtures with direct measurement of φ (no column).

the average delay due to the 0.1-min cycle time for the solenoid valves that feed the mixer. The extrapolated value of V_D' (equal to V_D) at $F = 0$ can be compared with the total volume of the gradient system, as summarized in Table II. The value of V_D measured from the geometry of the system is 5.48 ml, in good agreement with a value of 5.5 ± 0.1 ml from Fig. 4.

Solute pre-elution. Eqn. 19 or 20 can be used to anticipate significant changes in t_g as a result of solute pre-elution (partial elution by the volume V_D of starting mobile phase). If pre-elution effects are suspected for a given gradient separation, sample injection should be repeated at times zero and t_D. Any increase in t_g for early eluting solutes in the latter *vs.* the former separation is confirmation of solute pre-elution when sample is injected at $t = 0$.

The effects of sample pre-elution can be eliminated by injecting samples at time t_D rather than at the time the gradient is started.

Gradient dispersion

Gradients produced by the DuPont Model 8800 were measured as described

TABLE II

VOLUMES OF ELEMENTS WITHIN DUPONT MODEL 8800 GRADIENT SYSTEM (BETWEEN MIXER AND COLUMN INLET)

Element	Volume (ml)	Dispersion, V_i^2 (ml²)
Mixer	2.15	4.62
Pump:		
Cylinder	0.06	0.00
Tubing*	0.84	0.00–0.07**
Filter	0.40	0.00***
Additional		
tubing*	2.03	0.01–0.11**
Total	$V_d = 5.48$	$V_M = 4.63$–4.81 (2.15–2.19 ml)

* Inner diameter 0.030 in.
** Varies with flow-rate ($0.2 \leqslant F \leqslant 4.0$ ml/min).
*** Packed mixing-vessel; see text.

under Experimental and compared with calculated gradient shapes from eqns. 25 and 26. Values of V_G were varied from 2.5 to 40 ml and the flow-rate was varied from 0.5 to 2.0 ml/min. The value of V_D (5.5 ml) measured in Fig. 4 was assumed, and a best fit of φ vs. V to eqns. 25 and 26 gave $V_M \approx 2.0$ ml. The resulting agreement between experimental (points) and calculated (solid curve) gradient shapes is shown in Fig. 2a–c for V_G values of 40, 20 and 10 ml, respectively. In each instance the experimental data points fall within experimental error of the calculated curves from eqns. 25 and 26. As predicted by theory, the dispersion of the gradient by the system was independent of flow-rate, when t_G was varied to maintain V_G constant ($V_G = t_G F$). The best-fit value of V_M (2.0 ml) from these data can be compared with the value estimated from the system mixing elements (Table II), equal to 2.1–2.2 ml. The two numbers agree within the probable error of each.

Effect of gradient dispersion on t_g. The effect of gradient dispersion on solute retention in gradient elution is illustrated in Fig. 2e. For values of $(V - V_D)/V_G$ between 0.2 and 0.6, the gradient is shifted vertically by an average of 0.10 units in φ. Therefore, a solute eluting in this part of the gradient will elute earlier by a time equivalent to 0.1 unit in φ. That is, a value of $\delta\varphi_m = 0.1$ unit results in a value of $\delta\varphi = -0.1$ unit. More precisely, the value of $\bar{\varphi}$ for the solute represents its average mobile phase composition during migration along the column, and the corresponding value of $\delta\varphi_m$ in Table I for this value of $\bar{\varphi}$, or the equivalent value of $(V - V_D)/V_G$, should then define the error in t_g ($= -\delta\varphi$).

The above discussion argues for the relationship

$$\delta\varphi = -\delta\varphi_m \tag{33}$$

However, this conclusion seems less obvious for those parts of the gradient near the beginning ($V = V_D$) or the end ($V = V_G + V_D$) of the separation, because of severe curvature of distorted gradients in these regions. It was therefore of interest to examine this question from both a theoretical and an experimental standpoint. Numerical integration of model cases, as described in Appendix I, can be used to determine values of $\delta\varphi$ and $\bar{\varphi}$ for each example. The value of $\bar{\varphi}$ and of V_M/V_G in turn allows the determination of $\delta\varphi_m$ from Table I. Generalizing these calculations, we found that to a first approximation

$$\delta\varphi = -1.1\,\delta\varphi_m \tag{34}$$

Experimental data for the case of $\bar{\varphi} \geqslant 0.85$ (from the following paper[12]) are plotted in Fig. 5 and compared with eqn. 34 (solid line). These data points fall close to the line predicted by eqn. 34, and confirm that eqn. 34 is an adequate approximation for determining the error in t_g values as a result of gradient dispersion. As discussed in the following paper[12], there are other contributions to $\delta\varphi_m$ as a result of processes occurring within the column. However, these are generally minor for the case of $\bar{\varphi} > 0.85$, and the good correlation of experimental and calculated data points in Fig. 5 bears this out. The validity of eqn. 34 is further tested in the following paper[12], where experimental values of $\delta\varphi$ are compared with values calculated from eqn. 7a, which takes into account all contributions to error in calculated values of t_g from eqn. 10.
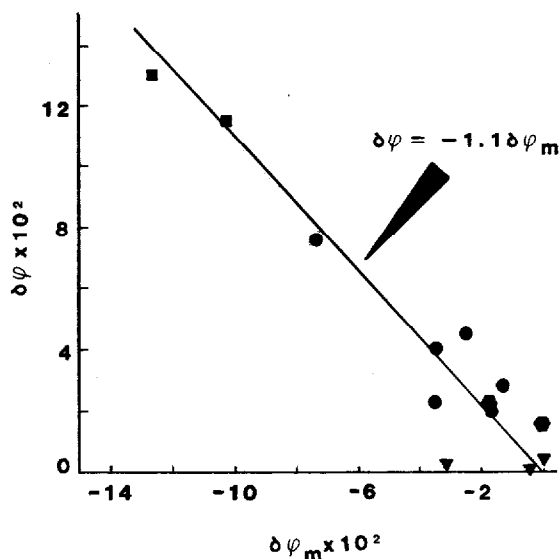
Fig. 5. Correlation of gradient dispersion ($\delta\varphi_m$) *vs.* change in solute retention ($\delta\varphi$). See text. V_G: ■, 5; ●, 10; ●, 16; ▼, 20 ml (experimental points); ——, best fit to calculated results (Appendix I).

Evaluation of new gradient systems

This study has adequately documented the gradient characteristics of the Du-Pont Model 8800 instrument. Other systems are expected to differ in the degree of gradient distortion, but not in the causes of gradient distortion. This study provides a basis for rapidly characterizing any new gradient system in terms of the important parameters V_D and V_M. Once these parameters are known for a given system, it is straightforward to predict deviations from ideal gradient shapes as a function of separation conditions *via* Table I. One approach is to calculate V_M and V_D as in Table II. Another approach is to begin with an estimate of V_M, which will generally be about equal to the volume of the gradient mixer. Next, two analog gradients are run (see Experimental) without a column, so as to display φ *vs.* time or volume V; values of V_M/V_G are selected to equal roughly 0.2 and 0.05. The latter gradient, which should show minimal dispersion, is used to determine V_D. In principle this latter step could be achieved by extrapolating the linear part of the analog gradient to $\varphi = 0$ (Fig. 2b), but in many instances the linearity of the gradient is deceptive, and this procedure leads to error in the estimated value of V_D. A better approach is to determine the value of the gradient time t for which $\varphi = 0.5$ ($t_{0.5}$). Then,

$$t_D = t_{0.5} - 0.5t_G \qquad (35)$$

Once t_D has been determined in this fashion, V_D is calculated as $t_D F$. The value of V_M can be estimated from the gradient with $V_M/V_G \approx 0.2$ by comparison of the gradient with the data in Table I. Specifically, the values of $\delta\varphi_m$ can be measured at times t_D and $t_D + t_G$ and averaged. This average value is equal to $(V_M/V_G)/2.72$, provided that V_M/V_G is not much greater than 0.2 (see Table I).

CONCLUSIONS

In this study we examined differences between actual and intended (ideal) gradients that result from non-ideality of the gradient system. General relationships were derived that allow calculation of mobile phase composition φ *vs.* gradient volume V for actual gradients; linear gradients were specifically considered here, but a similar approach can be used for other gradient shapes. Changes in gradient shape were considered as a result of (a) solvent misproportioning and flow-rate errors, (b) gradient delay due to the volume of the system between the mixer and the column inlet and (c) gradient distortion due to dispersion of the gradient within the system. Modern low-pressure gradient systems as exemplified by the DuPont Model 8800 used here will generally not be much affected by errors from solvent misproportioning or flow-rate effects. The effect of gradient delay on sample retention in gradient elution is easily corrected for, and measurement of the delay volume, V_D, for a particular system is straightforward. Gradient dispersion has a more complex effect on experimental t_g values, but these errors can also be corrected for, if the effective mixing volume V_M of the system is known. Generally V_M will approximate the volume of the gradient mixer, but its exact value can be experimentally determined as described here. Thus all effects leading to distortion or displacement of an actual gradient *vs.* the originally intended gradient can be determined for a given case, and the effect of these gradient distortions on solute retention t_g can be estimated. This allows the selection of preferred gradient systems and/or experimental conditions for minimum gradient distortion and minimum error in calculated values of t_g. Specifically, larger values of V_G (larger values of t_G and/or F) will give smaller values of V_M/V_G and therefore less gradient dispersion. Similarly, the calculation of isocratic retention data from gradient runs as in the following paper[12] can be made more precise by limiting gradient distortion and/or correcting for its effects.

We shall examine these effects further in the following paper[12], where precise predictions of t_g values will be shown for systems involving severely non-ideal gradients.

APPENDIX I

Calculation of $\delta\varphi$ as a function of $\bar{\varphi}$ and V_M/V_G
The effect of gradient distortion on values of t_g can be examined for specific cases by numerical integration of the fundamental equation for retention in gradient elution[1]:

$$\int_0^{V_g} (\mathrm{d}V/V_a) = 1 \tag{A1}$$

where V_g is the elution volume of the solute band in a gradient elution run and V_a is the instantaneous (isocratic) elution volume of the solute as a function of time during migration of the band along the column. V is the total volume of mobile phase that has passed through the band center at any given time. Eqn. A1 is com-

pletely general for any gradient shape, and can therefore be applied to the exact calculation of t_g values, even for very distorted gradients as in Fig. 2c and 2d.

Solution of eqn. A1 was achieved for several representative cases summarized in Fig. 5, with b taken equal to 0.3 in each instance. The solid curve in Fig. 5 is the best fit to these calculated values of $\delta\varphi$ vs. values of $\delta\varphi_m$ determined from Table I and values of $\bar{\varphi}$ calculated from eqn. A1.

REFERENCES

1 L. R. Snyder, in Cs. Horvath (Editor), *High-Performance Liquid Chromatography*, Vol. 1, Academic Press, New York, 1980, p. 207.
2 L. R. Snyder and J. J. Kirkland, *Introduction to Modern Liquid Chromatography*, Wiley-Interscience, New York, 2nd ed., 1979, Ch. 16.
3 J. J. Kirkland and J. L. Glajch, *Anal. Chem.*, 54 (1982) 2593; *J. Chromatogr.*, 255 (1983) 27.
4 P. J. Schoenmakers, H. A. H. Billiet and L. de Galan, *J. Chromatogr.*, 205 (1981) 13.
5 R. Lehrer, *LC Mag.*, 1, No. 2 (1983) 84.
6 J. P. Larmann, J. J. DeStefano, A. P. Goldberg, R. W. Stout, L. R. Snyder and M. A. Stadalius, *J. Chromatogr.*, 255 (1983) 163.
7 M. Martin and G. Guiochon, in J. F. K. Huber (Editor), *Instrumentation for High-Performance Liquid Chromatography*, Elsevier, Amsterdam, 1978, Ch. 3.
8 J. Korpi and B. A. Bidlingmeyer, *Amer. Lab.*, June (1981) 110.
9 H. A. H. Billiet, P. D. Keehnen and L. de Galan, *J. Chromatogr.*, 185 (1979) 515.
10 P. Jandera and J. Churacek, *Advan. Chromatogr.*, 19 (1980) 125.
11 R. P. W. Scott and P. Kucera, *J. Chromatogr.*, 185 (1979) 27.
12 M. A. Quarry, R. L. Grob and L. R. Snyder, *J. Chromatogr.*, 285 (1984) 19.
13 H. Engelhardt and H. Elgass, to be published.
14 S. T. Balke and R. D. Patel, *J. Liq. Chromatogr.*, 3 (1980) 741.
15 J. C. Sternberg, *Advan. Chromatogr.*, 2 (1966) 205.
16 K. Hoffman and I. Halász, *J. Chromatogr.*, 173 (1979) 211.
17 J. G. Atwood and M. J. E. Golay, *J. Chromatogr.*, 218 (1981) 97.